

Tunable ratchet effects for vortices pinned by periodic magnetic dipole arrays ^{*}

Gilson Carneiro ^a

^aInstituto de Física, Universidade Federal do Rio de Janeiro, C.P. 68528, 21941-972, Rio de Janeiro-RJ, Brasil

The ratchet effect is demonstrated theoretically for the simple model of a vortex in a thin superconducting film interacting with a periodic array of magnetic dipoles placed in the vicinity of the film. The pinning potential for the vortex is calculated in the London limit and found to break spatial inversion symmetry and to depend on the orientation of the magnetic dipole moments. The motion of the vortex at zero temperature driven by a force oscillating periodically in time is investigated numerically. Drift vortex motion consisting of displacements by a translation vector of the dipole array during each period of oscillation is obtained and studied in detail. The direction of drift differs in general from that of the driving force, except if the driving force oscillates in a direction of high symmetry of the dipole array. The vortex drift velocity depends on the orientation of the magnetic moments, and can be tuned by rotating the dipoles. It is pointed out that if the magnetic moments are free to rotate, the ratchet effect can be produced and tuned by a magnetic field applied parallel to the film surfaces.

1. Introduction

Possible applications of superconductivity to electronic devices based on the control of vortex motion has received a great deal of attention lately. One line of work uses vortex pinning by periodic potentials lacking spatial inversion symmetry to produce drift vortex motion in a preferred direction when driven by an oscillating force with zero average. This is the so called ratchet effect [1]. Applications to removal of trapped flux from superconductors, and to voltage rectification have been proposed [2,3,4,5,6,7]. Experimental realizations of the ratchet effect for vortices have been reported by some groups [8,9,10]. The work so far has concentrated on vortex pinning potentials resulting from periodic modulations of the film thickness or from periodic arrays of anti-dots or blind holes with asymmetric shape. The objective of this paper is to show that the ratchet effect can be obtained for vortices in thin superconducting films pinned by periodic arrays of magnetic dots placed in the vicinity of the film. Here a simple

model is studied in detail. One vortex in a thin superconducting film interacting with a periodic array of point magnetic dipoles, placed on top of the film in the London limit. The ratchet effect results from the interaction between the vortex and the magnetic dipole array if the magnetic moments are parallel to the film surfaces, and all moments point in the same direction. As shown here, the interaction between the vortex and the dipole array breaks inversion symmetry, and depends on the orientation of the magnetic moment with respect to the lattice. The latter allows the ratchet effect to be tuned by rotating the magnetic moments. If the dipole array is made of freely rotating magnetic moments, the ratchet effect can be produced and tuned by a magnetic field applied parallel to the film surfaces. This field orients all magnetic moments in the same direction, and does not influence the vortices because the film is thin. This may be of practical interest because it is possible to fabricate arrays with freely rotating magnetic moments, as demonstrated recently by Cowburn, et. al.[11]. These authors reported on the magnetic properties of arrays of nanomagnets made of Supermal-

^{*}Research supported in part by the Brazilian agencies CNPq, CAPES, FAPERJ, and FUJB.

loy, each nanomagnet being a thin circular disk of radius R , and found that for $R \sim 50 - 100\text{nm}$ the magnetic state of each nanomagnet is a single domain one, with the magnetization parallel to the disk plane, and that the magnetization can be re-oriented by small applied fields. They concluded that each nanomagnet acts like a giant magnetic moment free to rotate.

The calculations carried out in this paper start from the exact interaction potential in the London limit between a vortex in a thin superconducting film and the dipole array. The interaction potential depends on the orientation of the magnetic moments with respect to the dipole lattice and, in general, lacks spatial inversion symmetry. The equation of motion for the vortex driven by a force periodic in time is then solved numerically at zero temperature, both for sinus-wave and square-wave time dependencies. It is found that drift vortex motion takes place in such a way that during each period of oscillation the vortex displacement is equal to a translation vector of the dipole array. The vortex displacement is not, in general, in the direction of the driving force, and depends in a complicated way on the orientation of the magnetic moments and of the driving force with respect to the dipole lattice. The ratchet effects is, thus, two-dimensional in general. One-dimensional ratchet effects are obtained if the driving force oscillates in a direction of high symmetry of the dipole array lattice. In this case the vortex motion is found to be similar to that reported in the literature for particles interacting with one-dimensional ratchet potentials [1]. The vortex drifts in the direction of the driving force oscillation. Its displacement during each period of oscillation is a integer multiple of the dipole lattice period in this direction, and depends on the orientation of the magnetic moments with respect to the direction of the driving force. The paper argues that the results obtained for this simple model are applicable to thin low- T_c superconducting films, and can be extended to vortex lattices commensurate with the dipole array.

The paper is organized as follows. In Sec. 2 the interaction between the vortex and the dipole array is obtained. The motion of the vortex inter-

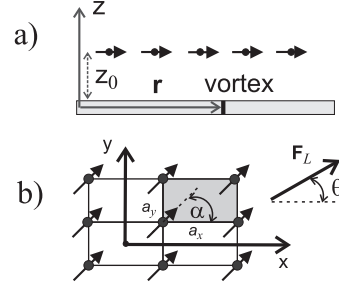


Figure 1. a) Schematic side view of the superconducting film with one vortex at \mathbf{r} and the dipole array on top. b) Top view of the dipole array, and definitions of angles α and θ

acting with the dipole array is examined in Sec. 3, where the main results of the paper are reported. Finally, Sec. 4 discusses the limits of validity of the model and its possible extensions, and states the conclusions of the paper.

2. Vortex- dipole array interaction

The superconductor film is assumed to be planar, with surfaces parallel to each other and to the $x - y$ plane, isotropic, characterized by the penetration depth λ , and of thickness $d \ll \lambda$. A plane dipole array is located above the film at a height $z_0 > 0$. The dipole array is characterized by a rectangular unit cell, with sides a_x and a_y , and one dipole per cell. All cells have the same magnetic moment, \mathbf{m} , parallel to the film surfaces, and oriented at an angle α with respect to the x -axis, as shown in Fig. 1. In the case of freely rotating magnetic moments, a magnetic field \mathbf{H} must be applied parallel to the film surfaces, at an angle α with the x -axis, in order to orient all magnetic moments in the same direction. The magnitude of the field must be large enough to avoid reorientation of the dipoles by the fields created by the vortex, by the other dipoles, and by the screening and transport currents flowing in the film [14]. The field \mathbf{H} does not influence the vortex, because the film is thin ($d \ll \lambda$).

The London limit interactions between vortices in superconducting films and magnetic dipoles located outside the film have been discussed in detail in Ref.[12], based on the exact solutions of London equations obtained in Ref.[13]. The interactions result from the action of the screening current induced by the inhomogeneous field generated by the dipoles on the vortices, and can be expressed as the magnetostatic interaction of the dipoles with the magnetic field generated by vortices. According to these results, the energy of interaction for a single vortex, with unity vorticity, located at position \mathbf{r} , and the dipole array, can be written as

$$U_{v-da}(\mathbf{r}) = - \sum_{j=1,N} \mathbf{m} \cdot \mathbf{b}_{\perp}^s(\mathbf{R}_j - \mathbf{r}) \quad (1)$$

where N is the number of dipoles in the array, \mathbf{R}_j their positions and \mathbf{b}_{\perp}^s is the component parallel to the film surfaces of the field generated by the vortex. The vortex field is given in the thin film limit and for $r \ll \Lambda = 2\lambda^2/d$ by [13]

$$\mathbf{b}_{\perp}^s(\mathbf{r}) = - \frac{\phi_0 d}{4\pi\lambda^2} \frac{\mathbf{r}}{r^2} \left(1 - \frac{z_0}{\sqrt{r^2 + z_0^2}}\right). \quad (2)$$

For $r > \Lambda$, $\mathbf{b}_{\perp}^s(\mathbf{r}) \sim \mathbf{r}/r^3$. For a periodic dipole array, the most important contribution to U_{v-da} comes from dipoles close to the vortex. The interaction between the vortex and a dipole located at distances larger than Λ from it behaves as $(\mathbf{R}_j - \mathbf{r})/|\mathbf{R}_j - \mathbf{r}|^3$, thus falling off as $1/R_j^2$ for $R_j \gg r$. However, the singular $1/R_j^2$ dependence is canceled out in the sum over dipoles present in Eq. (1) by symmetry. The leading contribution falls only as $1/R_j^3$. Here the contribution from far away dipoles is cutoff exponentially, as discussed shortly.

The vortex pinning potential can be written as the sum of contributions from each dipole, that is

$$U_{v-da}(\mathbf{r}) = - \sum_{j=1,N} \mathcal{U}(\mathbf{R}_j - \mathbf{r}), \quad (3)$$

where $\mathcal{U}(\mathbf{r})$ is the pinning potential for a single dipole located at the origin, and given by

$$\mathcal{U}(\mathbf{r}) = \frac{\phi_0 d}{4\pi\lambda^2} \frac{\mathbf{m} \cdot \mathbf{r}}{r^2} \left(1 - \frac{z_0}{\sqrt{r^2 + z_0^2}}\right) e^{-(r/\Lambda)}, \quad (4)$$

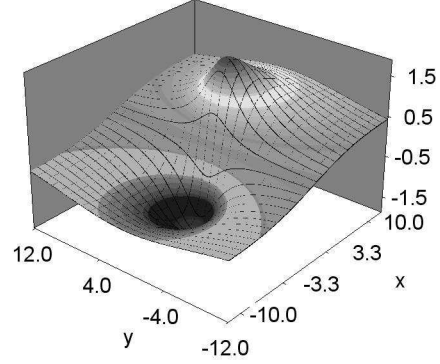


Figure 2. Vortex pinning potential (in units of $\epsilon_0 d = (\phi_0/4\pi\lambda)^2 d$) for a single dipole with \mathbf{m} parallel to the x -axis. x and y in units of ξ . Parameters: $m = 0.25\phi_0 z_0$, $d = z_0 = 2\xi$, $\lambda = 10\xi$.

where the exponential factor is the cutoff for the contributions from far away dipoles. According to Eq. (4), $\mathcal{U}(\mathbf{r})$ is anti-symmetric with respect to spatial inversion and has a minimum (maximum) located at $\mathbf{r} \cdot \hat{\mathbf{m}} = -(+)1.3z_0$. For \mathbf{m} oriented parallel to the x -axis, $\mathcal{U}(\mathbf{r})$ has the spatial dependence shown in Fig. 2.

For a dipole array $U_{v-da}(\mathbf{r})$ is the periodic repetition of \mathcal{U} , centered at each dipole. The spatial dependence of $U_{v-da}(\mathbf{r})$ for a typical rectangular dipole array is shown in Fig. 3 for some values of α .

The vortex-dipole array interaction $U_{v-da}(\mathbf{r})$ lacks spatial inversion symmetry and leads to the ratchet effect when the vortex is driven by an oscillating force, as discussed next.

3. Ratchet effects

The motion of a vortex in the potential $U_{v-da}(\mathbf{r})$, driven by a force $\mathbf{F}_L(t)$ is governed, at zero temperature, by

$$\eta \frac{d\mathbf{r}}{dt} = \mathbf{F}_L(t) - \nabla U_{v-da}(\mathbf{r}), \quad (5)$$

where η is the vortex friction coefficient. The driving force, $\mathbf{F}_L(t)$, results from a transport cur-

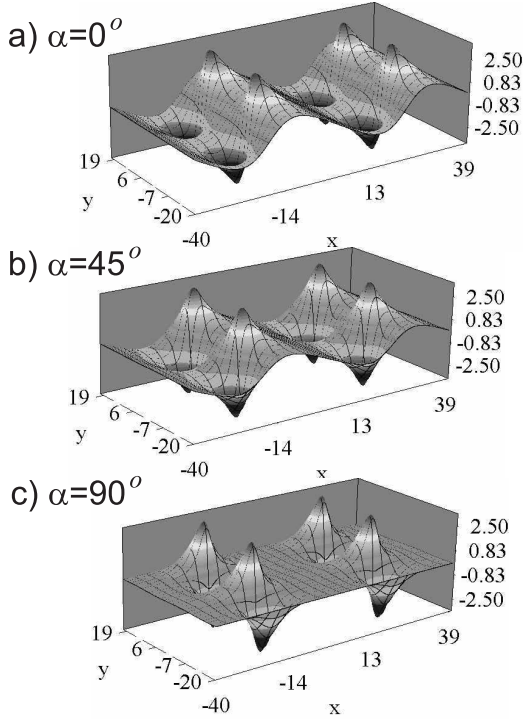


Figure 3. Vortex pinning potentials (in units of $\epsilon_0 d$) for dipole arrays with magnetic moments oriented at angle α with the x -axis. x and y in units of ξ =vortex core radius. Parameters: $m = 0.25\phi_0 z_0$, $d = z_0 = 2\xi$, $\lambda = 10\xi$.

rent density, $\mathbf{J}(t)$ applied to the film, that is $\mathbf{F}_L(t) = (\phi_0 d/c)\mathbf{J}(t) \times \hat{\mathbf{z}}$. The dipole array lattice is assumed rectangular with $a_x > a_y \gg z_0$. In this case $U_{v-da}(\mathbf{r})$ is like that shown in Fig. 3. It is convenient to use the following natural units for physical quantities. Length: ξ = vortex core radius. Force: $\epsilon_0 = (\phi_0/4\pi\lambda)^2$. Time: $\tau = \eta\xi/\epsilon_0$. Velocity: ϵ_0/η . Current density: $J_d = c\phi_0/(12\sqrt{3}\pi^2\lambda^2\xi)$, where J_d is the depairing current. When Eq. (5) is written in terms of these natural units it depends only on the scaled parameters $m/\phi_0 z_0$, d/z_0 , Λ/z_0 , J/J_d , and on $(\mathbf{R}_j - \mathbf{r})/z_0$. The values of J are, of course, lim-

ited to $J < J_d$, but in the results reported next regions where $J_c > J_d$ are discussed for the sake of completeness.

As will be seen shortly, the dc critical current to depin a vortex from a minimum of $U_{v-da}(\mathbf{r})$ plays an important role in the ratchet effect. To obtain it, Eq. (5) is solved for a time-independent transport current. The critical current depends, in general, on the orientations of \mathbf{m} and of the driving force with respect to the dipole lattice. In the case of interest here, $a_x, a_y \gg z_0$, it is found that the critical current is essentially identical to that for a vortex pinned by a single dipole, obtained in Ref. [14], and depends only on the angle between the dipole and the driving force, β . The critical current $J_c(\beta)$ is shown in Fig. 4. The maximum J_c occurs when \mathbf{m} is parallel to the direction of the driving force, $\beta = 0$, and the minimum for $\beta = 180^\circ$. There is a tenfold difference between the maximum and minimum values, and a smooth decrease in J_c with increasing β . The maximum and minimum J_c can be estimated analytically from the single dipole pinning potential, Eq. (4). The result is $J_c/J_d \simeq 4m/\phi_0 z_0$ for $\beta = 0$, and $J_c/J_d \simeq 0.4m/\phi_0 z_0$ for $\beta = 180^\circ$.

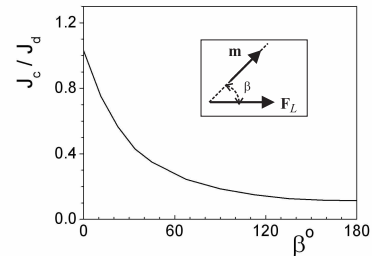


Figure 4. Critical current, J_c , for a vortex pinned by the dipole array vs. angle between the magnetic moments and the driving force, β (inset).

For an oscillating transport current with zero average, Eq. (5) is solved numerically and the vortex velocity averaged in time in the steady-state regime, denoted by \mathbf{V} , is calculated. Drift vortex motion occurs if $\mathbf{V} \neq 0$. The transport current is assumed to oscillate in a direction defined by the unit vector $\hat{\mathbf{n}}$, that makes an angle θ with the y -axis, and to be periodic in time with period P and zero average. Writing $\mathbf{J}(t) = J_T f(t) \hat{\mathbf{n}}$, J_T is the amplitude, and $f(t)$ is chosen as either as sinus wave, $f(t) = \sin(2\pi t/P)$, or as square wave, $f(t) = 1$ for $kP \leq t < (k+1/2)P$, and $f(t) = -1$ for $(k-1/2)P \leq t < kP$, with $k = 0, \pm 1, \pm 2, \dots$. The driving force oscillates in the direction perpendicular to $\hat{\mathbf{n}}$, which makes an angle θ with the x -axis (Fig. 1). It is found that for arbitrary θ the ratchet effect is two-dimensional (2D), with drift vortex motion taking place both in the directions parallel and perpendicular to $\mathbf{F}_L(t)$. The ratchet effect is one-dimensional (1D) only if $\theta = 0^\circ, 90^\circ$, that is, when $\mathbf{F}_L(t)$ oscillates along directions of high symmetry of the rectangular dipole lattice (x and y directions, respectively). In these cases drift vortex motion takes place only in the direction of the driving force.

Next the results of the numerical solution of Eq. (5) are reported for the following parameter values: $d = z_0 = 2\xi$, $\lambda = 10\xi$, $a_x = 20\xi$, $a_y = 40\xi$, $m = 0.25\phi_0 z_0$.

3.1. One-dimensional ratchet

Here the 1D ratchet effect is considered for $\theta = 0$, that is $\mathbf{F}_L(t)$ oscillating in the x -direction. In this case the vortex drifts only in the x -direction ($V_y = 0$), and V_x depends on J_T , α and P . Typical V_x vs. J_T curves for $0 \leq \alpha < 90^\circ$ are shown in Fig. 5. In this case the vortex drifts in the negative x -direction. For $90^\circ < \alpha \leq 180^\circ$, the vortex drifts in the positive x -direction, and the V_x vs. J_T curves are identical to those for $180^\circ - \alpha$ with V_x replaced by $-V_x$. For $\alpha = 90^\circ$ there is no drift vortex motion, and $V_x = 0$. The most important characteristics of the V_x vs. J_T curves for $0 \leq \alpha < 90^\circ$ are the following. Drift vortex motion only occurs if J_T is larger than a minimum value, denoted by $J_0(\alpha)$. For $J_T > J_0(\alpha)$ the V_x vs. J_T curves have two distinct regions: one for $J_0(\alpha) < J_T < J_m(\alpha)$, and another for

$J_T > J_m(\alpha)$, where $J_m(\alpha)$ denotes the value of J_T for which V_x is minimum ($|V_x|$ is maximum). It is found that in the region $J_0(\alpha) < J_T < J_m(\alpha)$ the vortex displacement during each period is an integer multiple of the lattice parameter a_x . The V_x vs. J_T curve consists of a series of plateaus where V_x is independent of J_T . In each plateau $V_x = \ell a_x / P$, $\ell = 1, 2, 3, \dots$. As shown in Fig. 5, the plateaus are clearly visible in the curve for $P = 1200\tau$. For $P = 24000\tau$ the plateaus are too narrow to be distinguished in the scale of the figure. For $J_T > J_m(\alpha)$, the V_x vs. J_T curve is strongly affected by the time dependence of the driving force. For the square wave, V_x drops to zero very quickly with J_T , while for the sinus wave V_x drops to zero slowly and is a complicated function of J_T . The dependence of V_x on α for fixed J_T is shown in the inset of Fig. 5.b, and will be discussed in more detail later. It is found that for both time dependencies $J_0(\alpha) \simeq J_c(180^\circ - \alpha)$ and $J_m(\alpha) \simeq J_c(\alpha)$. More details of the dependence of V_x on J_T , α and P is given next.

$\alpha = 0$: In the steady state regime there is no motion in the y -direction. The vortex moves only in negative x -direction, along a line connecting the minima of $U_{v-da}(\mathbf{r})$, for instance $y = a_y/2$ (see Fig. 3.a). Thus the vortex dynamics is one-dimensional in the potential $U_{v-da}(x, y = a_y/2)$ for $\alpha = 0$. As shown in Fig. 6, this 1D potential has characteristics similar to ratchet potentials used in other contexts [1]. For $J_0(0) < J_T < J_m(0)$ the vortex moves only during the half periods of oscillation when $\mathbf{F}_L(t)$ points in the negative x -direction. When $\mathbf{F}_L(t)$ points in the positive x -direction the vortex is pinned because $J_m(0) \simeq J_c(0)$ (see Fig. 4). For $J_T > J_m(0)$ the vortex moves both in the negative and positive x -directions, but the displacement is larger in the negative x -direction due to the lack of inversion symmetry of $U_{v-da}(x, y = a_y/2)$.

$0 < \alpha < 90^\circ$: Vortex motion is found to be two-dimensional, but drift takes place only along the negative x -direction. In the y -direction the vortex oscillates with zero average. Drift vortex motion is similar to that for $\alpha = 0$. For $J_0(\alpha) < J_T < J_m(\alpha)$ the vortex is pinned when $\mathbf{F}_L(t)$ points in the positive x -direction because $J_m(\alpha) \simeq J_c(\alpha)$. However, since $J_c(\alpha)$ decreases

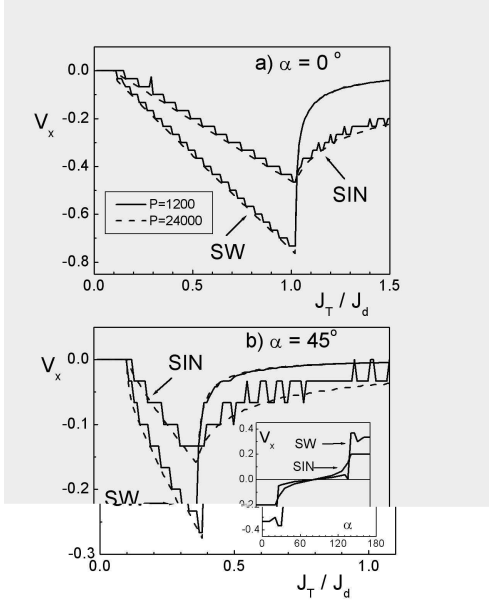


Figure 5. Vortex drift velocity (in units of ϵ_0/η) vs. J_T for driving force parallel to the x -axis ($\theta = 0$), and magnetic moments at an angle α with the x -axis. Labels: SIN and SW = sinus-wave and square-wave driving forces, respectively. Inset in b) V_x vs. α for $J_T = 0.5J_d$ and $P = 1200$. P in units of $\tau = \eta\xi/\epsilon_0$.

as α increases, the value of J_T for which V_x is minimum ($J_T = J_m(\alpha)$) decreases with α , and the value of V_x at the minimum increases ($|V_x|$ decreases) with α . As shown in the inset of Fig. 5.b, for J_T fixed, the value of V_x is weakly dependent on α as long as $J_T < J_m(\alpha)$. For $J_T > J_m(\alpha)$, V_x drops to zero rapidly with α . This result can be understood by noting first that the average slopes of the V_x vs. J_T curves in region $J_0(\alpha) < J_T < J_m(\alpha)$ are essentially independent of P , as shown in Fig. 5. Second, the average slope of the V_x vs. J_T curve is linear, except for J_T close to $J_0(\alpha)$, and weakly dependent on α . This occurs because the driving force is large compared with the pinning force in the direction of

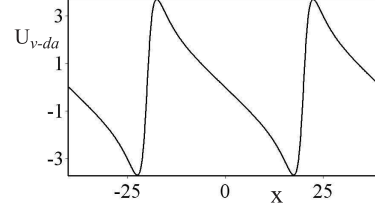


Figure 6. One-dimensional vortex pinning potential $U_{v-da}(x, y = a_y/2)$ (in units of $\epsilon_0 d$), for $\alpha = 0$. x in units of ξ

drift. An estimate for V_x in this case is obtained by neglecting the pinning force during the half period of oscillation where vortex drift motion takes place. The result is $V_x \sim -0.5J_T/J_d(\epsilon_0/\eta)$ for the sinus wave, and $V_x \sim -0.8J_T/J_d(\epsilon_0/\eta)$ for the square wave. These estimates are in reasonable agreement with the values of V_x shown in the inset of Fig. 5.b for $J_T < J_m(\alpha)$

Tuning the 1D ratchet effect is illustrated in the inset of Fig. 5.b. Basically, by rotating the magnetic moments the vortex drift velocity can be switched off, on, and reversed.

3.2. Two-dimensional ratchet

Now the 2D ratchet effect for $\theta \neq 0$ is considered. In this case \mathbf{V} depends both on θ and α , as well as on J_T , in a complicated way. Typical results for the dependence of \mathbf{V} on J_T and θ is shown in Fig. 7 and Fig. 8 for the square-wave driving force. The curves for V_x and V_y vs. J_T are similar to those obtained for $\theta = 0$. There is a value $J_T = J_0$ below which $V_x = V_y = 0$, and a value $J_T = J_m$ for which both V_x and V_y are minimum. It is found that $J_m \simeq J_c(|\theta - \alpha|)$, and $J_0 \simeq J_c(180^\circ - |\theta - \alpha|)$. For $J_0 < J_T < J_m$, the V_x vs. J_T and V_y vs. J_T curves show plateaux where both V_x and V_y are independent of J_T . Each plateau corresponds to a vortex displacement by a lattice translation vector, $\mathbf{R} = n_x a_x \hat{\mathbf{x}} + n_y a_y \hat{\mathbf{y}}$, $n_x, n_y = 0, \pm 1, \pm 2, \dots$. The direction of \mathbf{V} (angle γ with the x -axis) is not, in general, parallel to the direction of driv-

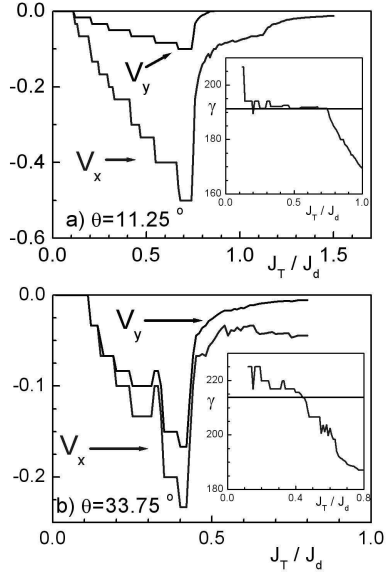


Figure 7. Vortex drift velocity components (in units of ϵ_0/η) vs. J_T for magnetic moments parallel to the x -axis ($\alpha = 0$), and square-wave driving force at angle θ with the x -axis and period $P = 1200\tau$. Insets: angle between the vortex drift velocity and x -axis, γ , vs. J_T . Horizontal lines: $\gamma = \theta + 180^\circ$.

ing force oscillation, as shown in the insets in Fig. 7 and Fig. 8. However, as shown in Fig. 7.a ($\alpha = 0, \theta = 11.25^\circ$) and Fig. 8.a. ($\alpha = 30^\circ, \theta = 15^\circ$), there are regions where the two directions nearly coincide ($\gamma = 180^\circ + \theta$). This occurs because for J_T in these regions the driving force is large compared to the pinning force during the drift vortex motion. Similarly to the case $\theta = 0$ discussed above, the average slopes of the V_x and V_y vs. J_T curves are linear in these regions. For $\alpha = 0, \theta = 33.75^\circ$, γ differs considerably from that of driving force oscillation. For $\alpha = 30^\circ, \theta = 30^\circ$, there is also a region where \mathbf{V} is parallel to the direction of drive, but the average slopes of the V_x vs. J_T and V_y vs. J_T curves are not linear. In this case the driving force os-

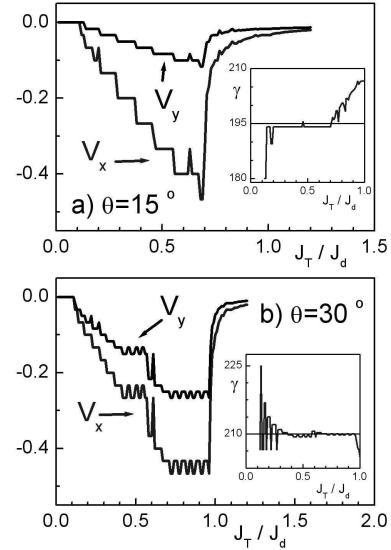


Figure 8. Vortex drift velocity components (in units of ϵ_0/η) vs. J_T for magnetic moments at $\alpha = 30^\circ$ with the x -axis, and square-wave driving force at angle θ with the x -axis and period $P = 1200\tau$. Insets: angle between the vortex drift velocity and x -axis, γ , vs. J_T . Horizontal lines: $\gamma = \theta + 180^\circ$.

cillates in a direction parallel to that of the magnetic moments, but the dependence of the drift velocity on J_T differs considerably from that for $\alpha = \theta = 0$. This shows that \mathbf{V} depends both on θ and α . Tuning of the vortex drift velocity by rotating the direction of the magnetic moments is also possible for $\theta \neq 0$. The dependence of V_x on α for fixed J_T is, essentially, similar to that shown in the inset of Fig. 5.b, since the V_x vs. J_T curves for $\theta \neq 0$ have the same basic structure as that for $\theta = 0$.

4. Discussion

First, an order of magnitude estimate of the vortex drift velocities obtained above is given.

Consider the case $\theta = 0$ and assume that $\xi = 20nm$, and $\eta = \eta_0 d$, with $\eta_0 = 7 \times 10^{-6} Nsm^{-2}$ [2]. In this case $d = z_0 = 2\xi = 40nm$, $\lambda = 10\xi = 200nm$ and $m = 0.25\phi_0 z_0 \sim 10^7 \mu_B$ ($\mu_B = \text{Bohr magneton}$). According to Sec. 3, the maximum values of $|V_x|$ are $|V_x|_{max} \sim 0.5J_c(\alpha)/J_d(\epsilon_0/\eta) \sim 10J_c(\alpha)/J_d m/s$ for the sinus wave and $|V_x|_{max} \sim 0.8J_c(\alpha)/J_d(\epsilon_0/\eta) \sim 16J_c(\alpha)/J_d m/s$ for the square wave. This gives for the sinus wave $|V_x|_{max} \sim 10m/s$ for $\alpha = 0$, and $|V_x|_{max} \sim 4m/s$ for $\alpha = 45^\circ$, and $|V_x|_{max} \sim 16m/s$ for $\alpha = 0$, and $|V_x|_{max} \sim 6m/s$ for $\alpha = 45^\circ$, for the square wave. These velocity values are of the same order of magnitude as those reported in Ref. [2]. The value of the unit time is $\tau = \eta\xi/\epsilon_0 \sim 10^{-9}s$. Thus, the transport current oscillation frequencies, $\nu = 1/P$, used in the calculations are $\nu = 800 KHz$, $40 KHz$ for $P = 1200\tau$, 24000τ , respectively.

The results obtained in this paper are believed to be representative of low- T_c superconducting films with magnetic dipole arrays placed on top. First, the particular set of parameters used, $d \sim z_0 \sim \xi$, are typical ones. For instance, in the experiments with arrays of magnetic dots with permanent magnetization placed on top of superconducting Nb films, reported in Ref.[15], $d = 20nm \sim \xi$. The magnetic dots are separated from the film by a thin protective layer of thickness $\sim 20nm$, so that the distance from the magnetic dipole to the film is $z_0 \sim \xi$. Second, since the vortex drift velocity depends on the scaled parameters $m/\phi_0 z_0$, d/z_0 , J/J_d , many superconducting film-dipole array systems are equivalent. Third, the results obtained in this paper do not depend on the particular dipole array used. What is essential for the ratchet effect is the periodic vortex pinning potential with broken spatial inversion symmetry created by it. Most dipole arrays will do, since the interaction between the vortex and a single dipole lacks inversion symmetry.

The London limit is valid for vortices in low- T_c films. However, when a magnetic dipole is placed close to the film, it certainly breaks down if the dipole field destroys superconductivity locally in the film. Roughly speaking, London theory is valid as long as the maximum dipole field at the film is less than the upper critical field, that is,

$m/z_0^3 < \phi_0/(2\pi\xi^2)$, or $m/(\phi_0 z_0) < (z_0/\xi)^2/2\pi$. For the parameters used in the above calculations ($z_0 = 2\xi$) this gives $m/(\phi_0 z_0) < 0.64$, which is larger than the value of m used in this paper. The London limit would be a better approximation if the present calculations were carried out for larger values of z_0/ξ . However, the results would be identical to those described above if m and d were scaled by the same factor as z_0/ξ . For instance, if $z_0 \rightarrow 2z_0$, J_c/J_d would remain the same if $d \rightarrow 2d$ and $m \rightarrow 2m$, but the upper limit of $m/\phi_0 z_0$ for the validity of the London approximation would increase by a factor of 4. The present model also breaks down if m is sufficiently large to create vortices in the film. The threshold value of m for spontaneous vortex creation, estimated as $m \sim 0.7\phi_0 z_0$ using the results of Ref.[12], is larger than m used here.

The results obtained in this paper for a single vortex also apply to vortex lattices pinned by dipole arrays if the vortex lattice is commensurate with the dipole array and if the vortex density is at most one vortex per dipole. In this case the driving force is expected to move the vortex lattice as a whole, that is preserving the spatial order, so that the effects of vortex-vortex interactions are negligible.

In conclusion then, this paper demonstrates the ratchet effect for vortices in a thin superconducting film pinned by periodic arrays of magnetic dipoles placed on top of the film, and shows that the ratchet effect can be tuned by rotating the magnetic moments. In the case of magnetic moments free to rotate, the ratchet is created and tuned by a magnetic film applied parallel to the film surfaces.

REFERENCES

1. For a recent review, see P. Reimann Phys. Rep. **361**, 57 (2002).
2. C.S.Lee, B.Jankó, L.Derényi, A.L.Barábasi, Nature **400**, 337 (1999).
3. I.Zapata, R.Bartussek, F.Sols, P.Hänggi, Phys. Rev. Lett. **77**, 2292 (1996).
4. J.F.Wambaugh, C.Reichhardt, C.J.Olson, F. Marchesoni, F.Nori, Phys. Rev. Lett. **83**, 5106 (1999).

5. B.Y.Zhu, F.Marchesoni, V.V.Moshchalkov, F.Nori, Phys.Rev.B **68** , 014514 (2003).
6. B.Y.Zhu, F.Marchesoni, F.Nori, Physica E **18**, 318 (2003).
7. S.Savel'ev, F.Nori, Nature Mater. **1**, 179 (2003).
8. J.E. Villegas, S.Savel'ev, F. Nori, E.M. Gonzalez, J.V. Anguita, R. García , J.L. Vicent, Science **302**, 1188 (2003).
9. J.E. Villegas, E.M. Gonzalez, M. P. Gonzalez, J.V. Anguita, J.L. Vicent, Phys. Rev. B **71**, 024519 (2005).
10. J. Van de Vondel, C. C. de Souza Silva, B. Y. Zhu, M. Morelle, and V. V. Moshchalkov, Phys. Rev. Lett. **94**, 057003 (2005).
11. R.P Cowburn, D.K. Kolstov, A.O. Adeyeye, and M.E. Welland, Phys. Rev. Lett. **83**, 1042 (1999).
12. G. Carneiro, Phys. Rev. B, **69** 214504 (2004).
13. G. Carneiro, and E.H. Brandt, Phys. Rev. B **61** 6370 (2000).
14. G. Carneiro, to appear in Europhys. Lett. .
15. Y. Otani, B. Pannetier, J. P. Nozières, and D. Givord J. Magn. Magn.Mater.**126**, 622 (1993); Y. Otani, Y. Nozaki, H. Miyajima, B. Pannetier, M. Ghidini, J. P. Nozières, G. Fillion, and P. Pagnat, Physica C **235 - 240**, 2945 (1994); Y. Nozaki, Y. Otani, K. Runge, H. Miyajima, B. Pannetier, J. P. Nozières, and G. Fillion, J. Appl. Phys**79**, 11 (1996).